On the Deployment of RIS-mounted UAV Networks[1]

A dissertation submitted in
partial fulfilment for the degree of

Master of Technology

in

Computer Science

by

Anupam Mondal
Roll No. - CS2304

Under the supervision of
Prof. Sasthi C. Ghosh
Advanced Computing and Microelectronics Unit
(ACMU)

INDIAN STATISTICAL INSTITUTE,
KOLKATA

June 2025

[*] ***This work has been submitted at The 33rd International Conference on Software, Telecommunications, and Computer Networks (SoftCOM 2025), to be held at Split, Croatia, during 18-20 September, 2025.***

[*] ***Preprint available at arXiv:2505.16841.***

Declaration

Anupam Mondal, with Roll No. **CS2304**, hereby declare that the material presented in the dissertation titled **On the Deployment of RIS-mounted UAV Networks** represents original work carried out by me for the degree of **Master of Technology in Computer Science** at the **Indian Statistical Institute, Kolkata**.
Furthermore, I affirm that no sections of this report have been sourced or copied from external references without proper attribution. I am aware that any instances of plagiarism or the use of unacknowledged materials from third parties will be treated with the utmost seriousness and consequences.

Anupam Mondal
M.Tech (CS), CS2304
Indian Statistical Institute
Kolkata – 700108, India

CERTIFICATE

This is to certify that the dissertation entitled **"On the Deployment of RIS-mounted UAV Networks"** submitted by **Anupam Mondal** to the **Indian Statistical Institute, Kolkata**, in partial fulfillment of the requirements for the degree of **Master of Technology in Computer Science**, is an authentic and genuine record of the research work carried out by the candidate under my supervision and guidance. I affirm that the dissertation has met all the necessary requirements in accordance with the regulations of this institute.

Prof. Sasthi C. Ghosh
ACMU Unit
Indian Statistical Institute
Kolkata – 700108, India

Acknowledgements

I extend my sincere appreciation to **Prof. Sasthi C. Ghosh**, my advisor at the *Advanced Computing and Microelectronics Unit* of the **Indian Statistical Institute, Kolkata**, for his guidance, continuous support, and inspiration. His profound knowledge and creative suggestions have taught me a lot about every subject and have shown me how to conduct solid research.

I would like to sincerely thank **Priyadarshi Mukherjee**, Senior Research Fellow at the **Indian Statistical Institute**, for his invaluable assistance in gathering the essential information for this research. His consistent provision of ideas and unwavering support have been instrumental in the success of this project.

I am deeply grateful to all the teachers at the **Indian Statistical Institute** for their invaluable advice, insight and instruction, which provided a crucial perspective for my research. Special thanks go to **Lakshmikanta Sau** and all the other seniors at the **MC (Mobile Computing Lab)** for their constant mentoring.

Finally, I want to express my gratitude to my parents and extended family for their unwavering support. I also extend my sincere appreciation to all my friends for their continuous assistance and encouragement. I am thankful to everyone who has contributed to my growth and success, even if I have inadvertently missed mentioning them on the above list.

Abstract

Reconfigurable intelligent surfaces (RIS) enable smart wireless environments by dynamically controlling signal propagation to enhance communication and localization. Unmanned aerial vehicles (UAVs) can act as flying base stations and thus, improve system performance by avoiding signal blockages. In this paper, we propose a gradient ascent and coordinate search based method to determine the optimal location for a system that consists of a UAV and a RIS, where the UAV serves cellular users (CUs) and the RIS serves device-to-device (D2D) pairs. In particular, by optimizing the net throughput for both the D2D pairs and the CUs, the suggested method establishes the ideal location for the RIS-mounted UAV. We consider both line of sight (LoS) and non-LoS (NLoS) paths for the RIS and UAV to calculate the throughput while accounting for blockages in the system. The numerical results show that the proposed method performs better than the existing approaches in terms of both the net throughput and the user fairness.

Keywords: Cellular users, device-to-device, reconfigurable intelligent surfaces, unmanned aerial vehicle, throughput, fairness.

Contents

List of Tables

List of Figures

List of Algorithms

Chapter 1

Introduction

Wireless communication systems have seen remarkable advances over the past few decades, evolving from basic voice transmission to high-speed data and multimedia services. With the rapid growth in data demand and the proliferation of connected devices, conventional terrestrial communication infrastructures are facing challenges in terms of scalability, adaptability, and efficiency. To meet the increasing requirements of future wireless networks, there is a growing interest in deploying intelligent and flexible communication architectures that can dynamically adapt to various environmental and network conditions.

Two emerging technologies that have attracted significant attention in this context are Unmanned Aerial Vehicle (UAV) and Reconfigurable Intelligent Surface (RIS). UAVs, due to their mobility, ease of deployment and ability to provide line-of-sight (LoS) connectivity, have emerged as a promising solution for enhancing coverage and capacity, especially in areas where terrestrial infrastructure is limited or unavailable. On the other hand, RIS are artificial surfaces composed of a large number of passive reflecting elements, which can smartly control the propagation of electromagnetic waves by altering their phase shifts. RIS can enhance signal strength, reduce interference, and improve the overall spectral and energy efficiency of wireless systems.

RIS represents a promising advancement in wireless communication systems. An RIS consists of a large number of low-cost, passive reflecting elements that can be programmed to control the direction, phase, and amplitude of electromagnetic waves. This ability allows RIS to reshape the wireless environment dynamically, enhancing signal strength, reducing interference, and improving the overall quality of communication links. In scenarios where obstacles such as buildings or walls cause signal blockage or degradation, RIS can effectively create alternative propagation paths, ensuring robust

and reliable connectivity. One of the key areas where RIS technology can have a significant impact is in Device-to-Device (D2D) communication. In D2D networks, users communicate directly without relying on the base station, which helps reduce latency and offloads traffic from the core network. However, D2D links are often vulnerable to poor channel conditions and interference from other users. By deploying RIS in such networks, the reflected signals can be adjusted to reinforce direct links between devices or to mitigate interference from surrounding transmissions. This leads to better link quality and improved spectral efficiency. Additionally, RIS is energy-efficient and flexible, making it well-suited for integration with mobile platforms like UAV, which can position the RIS elements in optimal locations depending on the network demand. When used in dynamic and dense network environments, such as urban areas, the combination of RIS and D2D communication can result in significant gains in throughput, fairness, and overall network performance. As the demand for high-speed and reliable communication grows, particularly with the development of 6G networks, RIS-assisted D2D systems are expected to play a crucial role in the evolution of future wireless technologies.

Cellular Users (CUs) are the standard users in a wireless network who rely on a base station or access point for communication. These users can be mobile phone users, IoT devices, or any terminal that connects to the cellular infrastructure to send or receive data. In dense urban areas or during peak hours, the communication quality for CUs can degrade due to congestion, interference, or poor signal coverage, especially in locations that are far from the base station or obstructed by buildings. To overcome these challenges, UAVs, also known as drones, are being increasingly used as aerial base stations or relay nodes in wireless networks. UAVs have the unique advantage of mobility, which allows them to be quickly deployed and positioned in the air to provide communication support where it is needed.

UAVs can help improve the coverage and capacity of a wireless network by establishing LoS links with ground users, thereby reducing the impact of obstacles and signal fading. When integrated with communication equipment, UAVs can either serve as temporary base stations or assist in relaying data between the users and the main network infrastructure. This is especially useful in emergency scenarios, rural areas with limited infrastructure, or events where a sudden increase in users leads to network overload. Moreover, UAVs can adjust their positions dynamically based on the user distribution or traffic demand, making the communication network more flexible and responsive. The combination of UAVs and ground-based CUs enables a more robust and adaptable network design, which is essential to support the growing demand for high-speed and reliable wireless communication services in next-generation networks.

Millimeter wave (mmWave) communication refers to the use of high-frequency radio waves, typically in the 30 to 300 GHz range, for wireless data transmission. This technology has gained significant attention in recent years, especially with the development of 5G networks, due to its ability to support extremely high data rates and large bandwidths. Unlike traditional cellular frequencies, mmWave signals can carry a much larger amount of data, making them ideal for applications that require fast and high-capacity communication, such as video streaming, virtual reality, and massive machine-type communications. However, despite its advantages, the mmWave technology also faces several challenges that must be addressed for practical use.

One of the main issues with mmWave is its limited range and high sensitivity to obstacles. These signals cannot easily penetrate walls, buildings, or even human bodies, and they are also affected by environmental factors such as rain and foliage. As a result, mmWave communication is heavily dependent on a clear LoS path between the transmitter and the receiver. When LoS is blocked, the signal must take alternative paths, known as Non-Line-of-Sight (NLoS) links. However, NLoS links typically suffer from higher path loss and signal degradation, leading to reduced performance. To overcome these limitations, advanced techniques such as beamforming, directional antennas, and intelligent reflecting surfaces (RIS) are used to redirect and enhance the signal strength, even in NLoS conditions. Moreover, deploying mmWave in dense urban areas often requires a higher density of base stations or the use of mobile platforms like UAVs to ensure stable and continuous coverage. Despite these challenges, mmWave technology holds great promise for future wireless networks by enabling ultra-fast, low-latency communication and supporting the growing demands of modern digital services.

The integration of RIS with UAV represents a novel and powerful paradigm for future wireless communication networks. By mounting RIS on UAV, we can harness the mobility and altitude advantages of UAV along with the signal manipulation capabilities of RIS, leading to highly reconfigurable and adaptive network deployments. This combination is especially beneficial in complex environments, such as urban areas with dense obstructions or remote locations that lack infrastructure support.

The main focus of this thesis is on the deployment of RIS-mounted UAV networks. Specifically, we aim to explore strategies for optimally positioning a UAV and a RIS to maximize network performance while serving both CUs and D2D communication pairs respectively. The motivation behind this research stems from the need to provide efficient and reliable connectivity in scenarios where traditional network setups are inadequate. By considering both UAV mobility and RIS reflection capabilities, we propose a framework that dynamically adjusts to user locations, obstacles, and channel conditions.

One of the primary challenges in deploying RIS-mounted UAV networks is determining the optimal positioning of both to support a heterogeneous user base. Unlike traditional base stations, UAV can move in three-dimensional space, and their positioning significantly influences the quality of the communication links. Furthermore, the placement of RIS on UAV adds an additional layer of complexity, as their effectiveness depends on the geometry of signal reflection paths. Thus, a comprehensive approach is needed to jointly consider user distribution, environmental factors, and communication requirements.

In this work, we propose a methodology for the deployment of RIS-mounted UAVs by formulating an optimization problem that aims to maximize a key performance metric such as network throughput or signal quality. We consider practical constraints such as the number of presence obstacles, the transmission power of devices, and the characteristics of wireless channels. Our approach involves simulating various scenarios and comparing the performance of our proposed method with existing benchmarks that consider UAVs or RISs separately.

However, since the RIS is mounted on the UAV, they have to be in the same location. Thus, in this work, we investigate the deployment aspect of RIS-assisted UAV networks, where our objective is to enhance the combined system throughput of both the CUs and the D2D pairs. More specifically, our contributions can be summarized as follows:

- First, we find the optimal position r_D of the RIS for maximizing the throughput of the D2D pairs based on gradient ascent, which may or may not be the best position with respect to the CUs.
- Next, we find the optimal position r_C of the UAV to maximize the throughput of the CUs, which again, may or may not be the best position for the D2D pairs.
- Finally, we find the combined optimal location of the RIS-mounted UAV based on coordinate search, by using r_D and r_C, which aims to maximize the net throughput of both the D2D pairs and the CUs.

We perform extensive simulations to demonstrate the benefits of the proposed method over the existing benchmark schemes, which individually optimizes the performance of the D2D pairs or the CUs. More precisely, our approach outperforms existing approaches in terms of both net throughput and user fairness.

The rest of the paper is organized as follows. Chapter 2 provides a detailed review of the related work in the area of UAV and RIS-assisted communication systems. It highlights the key contributions and limitations of existing approaches. Chapter 3 introduces the system model used in this study, including the overall network architecture and

assumptions made for the simulation. Chapter 4 presents the proposed method for determining the optimal placement of the RIS-mounted UAV, taking into account both CUs and D2D communication users.

Chapter 5 presents the simulation parameters used to evaluate the proposed system under various scenarios. Chapter 6 presents the simulation results and provides a performance comparison between our proposed approach and existing benchmark methods. Chapter 7 summarizes the key findings and insights obtained from the evaluation and concludes the thesis.

Chapter 2

Related Work

In recent years, wireless data usage has grown rapidly and is expected to increase more than five times between 2023 and 2028 [1]. In this context, RISs have emerged as a promising solution to tackle this challenge by 'controlling' the wireless propagation environment [2]. An RIS is essentially an array of passive elements placed on a flat metasurface. Unlike traditional methods that adapt to changes in the wireless channel, an RIS actively controls the wireless environment to improve signal transmission. This is achieved by adjusting the properties of its passive elements. Moreover, since an RIS only reflects the incoming signals in a desired direction, it does not require any radio frequency (RF) chains [3].

On the other hand, high-frequency signals such as millimeter waves (mmWaves) [4] are widely used for high-speed data transfer in the D2D communication. Although mmWaves-based communication is well suited for short-distance D2D communication, it comes with its own set of challenges such as losing signal strength quickly when passing through obstacles and experiencing high signal loss over long distances. These limitations make it difficult to always maintain a stable and strong connection between a user pair, especially in situations where the direct LoS is weak or not good enough to support mmWave communication. In such scenarios, RIS-assisted D2D communication can help obtain the indirect LoS when the direct LoS is blocked [5].

Using an RIS, the signal can be intelligently reflected and redirected to the desired destination, even when obstacles block the direct path. This helps ensure a more reliable and efficient wireless connection. Furthermore, to make communication more reliable, RIS is placed in a strategic location where they have a clear LoS with the users who want to communicate with each other. This is crucial, since there is a significant difference in between the LoS and NLoS path loss (PL) in mmWave communication. NLoS

communication occurs when buildings or other obstacles block the direct signal path, leading to higher signal loss and weaker connections. Moreover, this strategic placement helps to improve signal quality and overall network performance [6, 7, 8]. In this setup, the signal from one user is reflected by an RIS placed within its communication range before reaching the intended receiver. This improves network connectivity, especially in areas where the direct LoS link is weak or blocked by obstacles.

In addition, for situations such as natural disasters and/or temporary high-traffic areas, UAV-aided communication can be a very useful alternative, where the traditional existing infrastructure may be unavailable or overloaded. UAVs are widely used in such cases because they offer high flexibility, quick and easy deployment, making them an effective solution for emergency and temporary communication needs [9]. As a result, UAVs, like RIS, can aid mmWave communication systems to avoid signal blockages and significantly reduce the associated PL [10]. Since UAVs can move freely and adjust their positions, they can find the best locations to maintain a LoS link, ensuring a more stable and reliable connection. In this context, a potential RIS-aided UAV network can deal with the blockage problem more efficiently [11]. Here the UAV can act as a flying base station to CUs and the RIS on top of it can help establish LoS links between the mmWave-based D2D user pairs. Because the RIS-assisted UAV network serves both types of users, this increases the system throughput. But in that case, the placement of the RIS-mounted UAV is a very challenging issue. Unlike the thoroughly investigated research direction of optimal UAV [12] and RIS [13] positioning, here we need to consider the net performance of both the CUs and the D2D pairs. It is important to note that the optimal UAV position corresponding to the CUs may or may not be the same as the optimal RIS position corresponding to the D2D pairs, and vice-versa.

Chapter 3

System Model

In this section, we explain the network setup and how the system works. We first describe the structure of the network, including the positions and roles of the UAV, the RIS, and the different users such as the CUs and D2D user pairs. This helps to understand how these components are arranged and how they interact with each other. After describing the network layout, we provide the mathematical model that represents the system. This includes the assumptions we make, the types of communication channels considered, and the important parameters used in our analysis. This model forms the basis for developing and evaluating our proposed method.

3.1 Network Topology

We consider a mmWave wireless system with N active CUs, M D2D pairs, and a RIS-mounted UAV that operates in the orthogonal frequency division multiple access (OFDMA) mode [14]. The RIS is made up of R reflecting patches and the UAV flies at a fixed altitude H above the ground level [15]. Also, we assume that the RIS is able to obtain complete channel state information (CSI) and that the wireless channels corresponding to the consecutive reflecting elements are independent and identically distributed. We denote $C = \{1, 2, \ldots, N\}$ and $D = \{1, 2, \ldots, M\}$ as the index sets for active CUs and D2D pairs, respectively. In addition, we assume $\{(x_1, y_1), (x_2, y_2), \ldots, (x_M, y_M)\}$ is the set of M D2D pairs communicating via the RIS and $\{z_1, z_2, \ldots, z_N\}$ is the set of N CUs, which communicate with the UAV as a base station. So, we have $K = 2M + N$ devices that communicate simultaneously.

Figure 3.1 illustrates a representative scenario of the proposed communication system architecture. In this setup, two CUs, denoted as z_1 and z_2, are engaged in data communication with a UAV that acts as an aerial base station. At the same time, two D2D

user pairs, represented as (x_1, y_1) and (x_2, y_2), establish direct communication with the assistance of a RIS. The RIS is mounted on the UAV, enabling intelligent signal reflection to support users in environments with obstacles or NLoS conditions. This figure provides a visual overview of how different types of users interact through the UAV and RIS, showcasing the hybrid nature of the network and the effectiveness of integrating advanced wireless communication technologies.

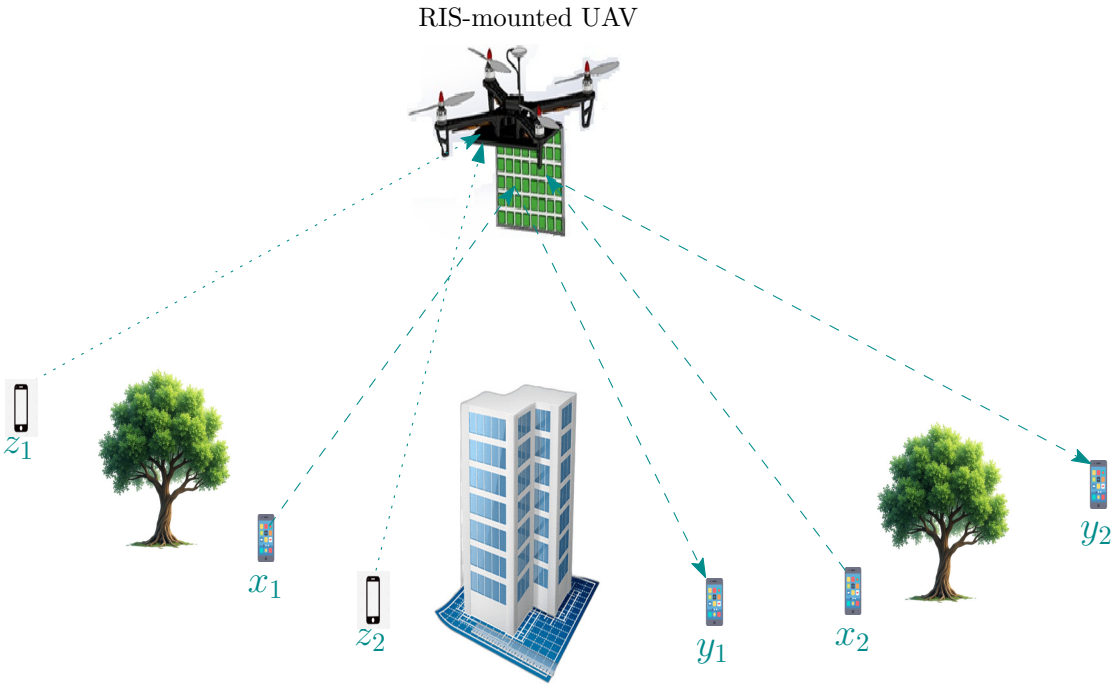

Figure 3.1: RIS-mounted UAV communication model.

3.2 Throughput Calculation for D2D Pairs

For $x_m \; \forall \; m = 1, \ldots, M$, the received signal at y_m is

$$s_{y_m} = \sqrt{P_{y_m}} \left[\sum_{\zeta=1}^{R} |h|_{m,\zeta} e^{-j\psi_{m,\zeta}} a_\zeta |g|_{m,\zeta} e^{-j\phi_{m,\zeta}} \right] s_m + n_o, \tag{3.1}$$

where P_{y_m} is the path loss dependent received power, s_m is the transmitted signal, and $n_o \sim \mathcal{CN}(0, N_0)$ denotes the additive white Gaussian noise (AWGN). Here, $a_\zeta = \omega_\zeta e^{j\theta_\zeta}$ $\forall \; \zeta = 1, \ldots, R$ is the reflection coefficient of the ζ-th RIS reflecting element and $\omega_\zeta(\theta_\zeta)$ denotes the amplitude (phase) adjustment factor of the same. Without any loss of

generality, we consider $\omega_\zeta = 1 \; \forall \; \zeta$ [5]. Moreover, $|h|_{m,\zeta}(\psi_{m,\zeta})$ and $|g|_{m,\zeta}(\phi_{m,\zeta})$ denote the amplitude (phase) of the channel coefficient of the $x_m - R$ link and the $R - y_m$ link, respectively. Furthermore, P_{y_m} depends on the PL model considered [16] as follows.

$$P_{y_m}[\text{dBm}] = P_{x_m} + G_{x_m} + G_{y_m} - PL_{x_m,RIS} - PL_{RIS,y_m}. \tag{3.2}$$

Here, P_{x_m} is the transmit power of x_m, $G_{x_m}(G_{y_m})$ is the gain of the transmit (receive) antenna, and

$$\begin{aligned} PL_{x_m,RIS} &= \alpha_{x_m,RIS} + 10\beta_{x_m,RIS}\log_{10}(d(x_m,r)) \text{ and} \\ PL_{RIS,y_m} &= \alpha_{RIS,y_m} + 10\beta_{RIS,y_m}\log_{10}(d(r,y_m)), \end{aligned} \tag{3.3}$$

where α and β are parameters of the LoS and NLoS models respectively, $d(x_m, r)$ is the Euclidean distance between x_m and RIS, and $d(r, y_m)$ is the Euclidean distance between RIS and y_m. Lastly, $|h|_{m,\zeta}$ and $|g|_{m,\zeta}$ follow the Rician or Rayleigh distribution, depending on whether they correspond to the LoS or NLoS channel, respectively[8]. As we assume the RIS to have the complete CSI, the resulting optimal signal at y_m is

$$s_{y_m} = \sqrt{P_{y_m}} \left[\sum_{\zeta=1}^{R} |h|_{m,\zeta}|g|_{m,\zeta} \right] s + n_o \tag{3.4}$$

and the associated total throughput for all the D2D pairs is

$$D_{\text{D2D}} = \sum_{m=1}^{M} \log_2 \left(1 + \frac{P_{y_m} \left| \sum_{\zeta=1}^{R} |h|_{m,\zeta}|g|_{m,\zeta} \right|^2}{N_0} \right). \tag{3.5}$$

3.3 Throughput Calculation for CUs

For $z_n \; \forall \; n = 1, \ldots, N$, the received signal at the UAV is

$$s_{z_n} = \sqrt{P_n} f_n s_n + n_o, \tag{3.6}$$

where P_n, analogous to P_{y_m} in (3.1), is the distance dependent received power, i.e., it is a function of $d(z_n, r)$ as follows.

$$P_n[\text{dBm}] = P_{z_n} + G_{z_n} + G_{UAV} - PL_{z_n,UAV}. \tag{3.7}$$

Here, P_{z_n} is the transmit power of z_n, $G_{z_n}(G_{UAV})$ is the gain of the transmit (UAV) antenna, and

$$PL_{z_n,UAV} = \alpha + 10\beta \log_{10}(d(z_n, r)). \tag{3.8}$$

Also, f_n is the corresponding complex channel gain, and s_n is the transmitted signal. Accordingly, the associated total throughput for all the CUs is given by

$$D_{\text{CU}} = \sum_{n=1}^{N} \log_2 \left(1 + \frac{P_n |f_n|^2}{N_0}\right). \tag{3.9}$$

Similar to $|h|_{m,\zeta}$ and $|g|_{m,\zeta}$ of the D2D scenario, $|f_n|$ is Rician/Rayleigh distributed depending on the wireless channel.

In this manuscript, we investigate the RIS-mounted UAV deployment, where we intend to maximize the net throughput D_{net}, which is defined from (3.5) and (3.9) as

$$D_{\text{net}} = D_{\text{D2D}} + D_{\text{CU}}. \tag{3.10}$$

Chapter 4

Proposed Strategy

In this section, we introduce a step-by-step strategy to maximize (3.10), which is the net throughput of the CUs and the D2D users. Specifically, we intend to individually maximize D_{D2D} and D_{CU} as two different sub-problems, by finding the best possible solution for each. Subsequently, by taking the solutions from both and combining them, we solve the original optimization problem. The motivation for this approach lies in the fact that, since the RIS is mounted on the UAV, we cannot have different locations for the RIS and the UAV in order to serve the D2D pairs and the CUs, respectively.

4.1 Throughput Maximization for D2D Pairs

Now, we obtain insights on the optimal placement of the RIS, which results in the maximization of D_{D2D}. Here, $D_{\mathrm{D2D}}(r)$ from (3.5), can be expressed as a function of the position of the RIS, i.e., $r = (x_r, y_r, H)$ as

$$D_{\mathrm{D2D}}(r) = \sum_{m=1}^{M} \log_2 \left(1 + \frac{P_{y_m}(r) \left| \sum_{\zeta=1}^{R} |h|_{m,\zeta} |g|_{m,\zeta} \right|^2}{N_0} \right), \tag{4.1}$$

where from (3.2), we have

$$P_{y_m}(r)[\mathrm{dBm}] = P_{x_m} + G_d - PL_{x_m,RIS} - PL_{RIS,y_m},$$

$G_d = G_{x_m} + G_{y_m}$, and $PL_{x_m,RIS}, PL_{RIS,y_m}$ as stated in (3.3). Note that, while P_{x_m} and G_d are constants, $PL_{x_m,RIS}$, PL_{RIS,y_m} depend on r and hence, P_{y_m} is a function of r. Thereafter, by appropriate linearization (i.e, conversion from dBm to Watt) of

$$D'_{D2D}(r) = \sum_{m=1}^{M} \frac{-\eta_m A_m}{(\ln 2)\left(1+\eta_m d(x_m,r)^{-\beta_{x_m,RIS}} d(y_m,r)^{-\beta_{RIS,y_m}}\right)}, \text{ where} \tag{4.4}$$

$A_m = \beta_{x_m,RIS} d(x_m,r)^{-\beta_{x_m,RIS}-1} d'(x_m,r) d(y_m,r)^{-\beta_{RIS,y_m}} + \beta_{RIS,y_m} d(x_m,r)^{-\beta_{x_m,RIS}} d(y_m,r)^{-\beta_{RIS,y_m}-1} d'(y_m,r).$

$P_{y_m}(r)$ and denoting $\left| \sum_{\zeta=1}^{R} |h|_{m,\zeta} |g|_{m,\zeta} \right|^2 = \kappa_m$, (4.1) can be rewritten as

$$\begin{aligned} D_{\mathrm{D2D}}(r) &= \sum_{m=1}^{M} \log_2 \left(1 + \frac{P_{y_m}(r)\kappa_m}{N_0}\right) \\ &= \sum_{m=1}^{M} \log_2 \left(1 + \eta_m d(x_m,r)^{-\beta_{x_m,RIS}} d(y_m,r)^{-\beta_{RIS,y_m}}\right), \end{aligned} \tag{4.2}$$

where $\eta_m = \frac{\kappa_m}{N_0} 10^{\frac{P_{x_m} + G_d - \alpha_{x_m,RIS} - \alpha_{RIS,y_m} - 30}{10}}$. Accordingly, by using (4.2), we state the following optimization problem.

$$\mathrm{P1}: \quad \max_{r} \quad D_{\mathrm{D2D}}(r) \tag{4.3}$$

subject to $x_{r_{\min}} \leq x_r \leq x_{r_{\max}}$ and $y_{r_{\min}} \leq y_r \leq y_{r_{\max}}$. To solve P1, we first calculate $D'_{\mathrm{D2D}}(r) = \frac{\partial D_{\mathrm{D2D}}(r)}{\partial r}$ to obtain (4.4). However, if we set $D'_{D2D}(r) = 0$ and try to solve for r, we do not get a closed-form solution. Therefore, we employ a numerical technique to find the best possible value of r.

Specifically, as $\log_2(\cdot)$ is a continuous and concave function, it has a global maximum point. Hence, we propose a gradient ascent [17] based algorithm, which will converge to this maximum point.

4.1.1 Gradient Ascent

Gradient ascent is a fundamental optimization algorithm used to maximize a function by iteratively moving in the direction of its gradient. It is especially useful in machine learning, data science, and mathematical modeling, where the goal is often to find the parameters that maximize a certain objective function, such as a likelihood function or a utility function.

Let $f(\mathbf{x})$ be a differentiable real-valued function, where $\mathbf{x}$ is a vector of parameters. The gradient of f, denoted by $\nabla f(\mathbf{x})$, is a vector of partial derivatives that points in the direction of the steepest increase of the function. In gradient ascent, we update the

parameters using the following rule:

$$\mathbf{x}_{t+1} = \mathbf{x}_t + \eta \nabla f(\mathbf{x}_t), \tag{4.5}$$

where $\eta > 0$ is the learning rate or step size, and t denotes the iteration number.

The learning rate η plays a crucial role in the convergence behavior of the algorithm. If η is too small, the algorithm may take a long time to converge. If it is too large, the algorithm may overshoot the maximum and fail to converge or even diverge. In practice, techniques such as adaptive learning rates or line search methods are used to address this issue.

Gradient ascent is widely applied in scenarios where an objective function needs to be maximized. For example, in logistic regression, the likelihood of the observed data is maximized with respect to model parameters. Similarly, in reinforcement learning, agents use gradient ascent to maximize the expected reward by adjusting their policy parameters.

Despite its simplicity, gradient ascent has some limitations. It requires the function to be differentiable and may get stuck in local maxima if the function is non-convex. To overcome this, various advanced techniques such as stochastic gradient ascent, momentum-based methods, and second-order methods (e.g., Newton's method) have been developed.

In summary, gradient ascent is a simple yet powerful optimization technique that plays a central role in many machine learning and statistical applications. Its effectiveness depends on careful tuning of parameters and, in complex problems, the use of extensions or variants to ensure better performance and convergence properties.

Accordingly, Algorithm 1 solves P1, where we avoid $r = x_m$ and y_m for all $m = 1, 2, \ldots, M$. We simply cannot take the gradient at $r = x_m$ and y_m for all $m = 1, 2, \ldots, M$ because the objective function is not defined at these points. To handle this, we define $\text{sign}(x) = +1$ for $x > 0$ and -1, elsewhere. Also, a small tolerance ϵ is used, i.e., if $d(x_m, r)$ or $d(r, y_m)$ is less than ϵ, we adjust r by moving it away from x_m and y_m $\forall$ m by a displacement factor δ. Furthermore, the bounds of r are carefully maintained by continuously adjusting its value after each update, making sure that it remains within the specified limits. In (4.3), we determine the limits of r as $r_{\min} = (x_{r_{\min}}, y_{r_{\min}}, H)$, $r_{\max} = (x_{r_{\max}}, y_{r_{\max}}, H)$, and we denote the initial value of r as $r_0 = (x_{r_0}, y_{r_0}, H)$. Here $r_{\min}$ and $r_{\max}$ are obtained so that after these points the PL is greater than the PL at r_0 [16]. Finally, the algorithm stops if

- The derivative of $D_{D2D}(r)$ evaluated at any iteration is less than ϵ, or

- The distance between two consecutive locations is less than ϵ, or
- The maximum number of iterations is reached.

The computational complexity of the proposed algorithm is influenced by two primary factors: the total number of D2D user pairs and the maximum number of iterations the algorithm is allowed to run. Here, M is the total number of D2D pairs in the network, and $N_{\max}$ is the maximum number of times the algorithm runs. In the worst case, the algorithm might need to process all user pairs during each round. As a result, the worst-case time complexity of the algorithm can be expressed as $\mathcal{O}(M \cdot N_{\max})$. This indicates that the execution time of the algorithm increases linearly with both the number of D2D users and the number of iterations. Such a complexity ensures that the algorithm remains scalable and efficient for moderate to large network sizes, making it practical for real-world deployment scenarios involving RIS-assisted UAV communications.

Algorithm 1 Algorithm to Solve P1

Initialize with initial guess r_0 such that $r_{\min} < r_0 < r_{\max}$ and $r_0 \neq x_m, y_m \ \forall \ m$, learning rate α, tolerance ϵ, and maximum iterations $N_{\max}$.
Set iteration count $k = 0$.
repeat
    Compute $D'_{\text{D2D}}(r)$ by using (4.4).
    $r_{k+1} = r_k + \alpha D'_{\text{D2D}}(r_k)$
    for all m **do**
        if $|r_{k+1} - x_m| < \epsilon$ **then**
            $r_{k+1} = r_{k+1} + \text{sign}(r_{k+1} - x_m) \cdot \delta$
        end if
        if $|r_{k+1} - y_m| < \epsilon$ **then**
            $r_{k+1} = r_{k+1} + \text{sign}(r_{k+1} - y_m) \cdot \delta$
        end if
    end for
    Ensure bounds: $r_{k+1} = \min(\max(r_{k+1}, r_{\min}), r_{\max})$
    $k = k + 1$
until $|D'_{\text{D2D}}(r_{k+1})| < \epsilon$ or $|r_{k+1} - r_k| < \epsilon$ or $k \geq N_{\max}$
return $r^* = r_{k+1}$ and $D_{\text{D2D}}(r^*)$

4.2 Throughput Maximization for CUs

Now we define an optimization problem specifically for the purpose of maximizing D_{CU}. Here, $D_{\text{CU}}(r)$ from (3.9), is expressed as

$$D_{\text{CU}}(r) = \sum_{n=1}^{N} \log_2 \left(1 + \frac{P_n(r)|f_n|^2}{N_0}\right), \tag{4.6}$$

where from (3.7), we obtain

$$P_n[\text{dBm}] = P_{z_n} + G_c - PL_{z_n,UAV}, \tag{4.7}$$

$G_c = G_{z_n} + G_{UAV}$, and $PL_{z_n,UAV}$ as stated in (3.8). By performing similar algebraic manipulations as in Section III-A, we obtain

$$D_{\text{CU}}(r) = \sum_{m=1}^{M} \log_2 \left(1 + \lambda_n d(z_n, r)^{-\beta_{z_n,UAV}}\right), \tag{4.8}$$

where $\lambda_n = \frac{|f_n|^2}{N_0} 10^{\frac{P_{z_n} + G_c - \alpha_{z_n,UAV} - 30}{10}}$. Similar to (4.3), we frame the following optimization problem.

$$\text{P2}: \quad \max_{r} \quad D_{\text{CU}}(r) \tag{4.9}$$

subject to $x_{r_{\min}} \leq x_r \leq x_{r_{\max}}$ and $y_{r_{\min}} \leq y_r \leq y_{r_{\max}}$.

Due to the similar structure of D_{CU} and D_{D2D}, here too we cannot find a closed-form optimal solution. Accordingly, on similar lines, we evaluate the quantity

$$D'_{\text{CU}}(r) = \sum_{n=1}^{N} \frac{-\lambda_n \beta_{z_n,UAV} d(z_n, r)^{-\beta_{z_n,UAV}-1} d'(z_n, r)}{(\ln 2)\left(1 + \lambda_n d(z_n, r)^{-\beta_{z_n,UAV}}\right)} \tag{4.10}$$

to propose Algorithm 2 for finding the best possible solution numerically.

Similarly, the optimization process for CUs, the computational complexity is influenced by the total number of CUs and the number of iterations allowed. Since N represents the number of CUs in the network, and $N_{\max}$ denotes the maximum number of iterations, in the worst-case scenario, the algorithm evaluates each CU in every iteration, leading to a time complexity of $\mathcal{O}(N \cdot N_{\max})$. This expression indicates a linear increase in computational cost with respect to the number of cellular users and the iteration count, thereby ensuring that the proposed approach remains scalable and efficient even in dense cellular network deployments.

It is interesting to note that, while Algorithm 1 depends on the location of both the users of every D2D pair, Algorithm 2 depends solely on the location of all the CUs.

4.3 Best Combined Position for RIS and UAV

By solving P1, Algorithm 1 determines the optimal position for the RIS to serve the current set of requesting D2D pairs. Similarly, Algorithm 2 provides solution to P2, to determine the best possible position for the UAV to serve as many CUs as possible. However, in general, these optimal positions obtained from Algorithm 1 and Algorithm

Algorithm 2 Algorithm to Solve P2

Initialize with initial guess r_0 such that $r_{\min} < r_0 < r_{\max}$ and $r_0 \neq z_n$ for all n, learning rate α, tolerance ϵ, and maximum iterations $N_{\max}$.
Set iteration count $k = 0$.
repeat
    Compute $D'_{\mathrm{CU}}(r)$ by using (4.10).
    $r_{k+1} = r_k + \alpha D'_{\mathrm{CU}}(r_k)$
    for all n **do**
        if $|r_{k+1} - z_n| < \epsilon$ **then**
            $r_{k+1} = r_{k+1} + \mathrm{sign}(r_{k+1} - z_n) \cdot \delta$
        end if
    end for
    Ensure bounds: $r_{k+1} = \min(\max(r_{k+1}, r_{\min}), r_{\max})$
until $|D'_{\mathrm{CU}}(r_{k+1})| < \epsilon$ or $|r_{k+1} - r_k| < \epsilon$ or $k \geq N_{\max}$
return $r^* = r_{k+1}$ and $D_{\mathrm{CU}}(r^*)$

2, respectively, are not the same. If we move away from these individually optimal positions, it is expected that the data rate for both D2D users and CUs will decrease. However, since the RIS is mounted on the UAV, we are interested in finding its joint optimal or 'near-optimal' position such that the reduction in data rate remains minimal. This is achieved by using the following approach.

Let the optimal position of RIS obtained by Algorithm 1 is r_{D}. The corresponding average throughput per D2D pair is defined as

$$D^{\mathrm{avg}}_{\mathrm{D2D}}(r_{\mathrm{D}}) = \frac{D_{\mathrm{D2D}}(r_{\mathrm{D}})}{M}. \tag{4.11}$$

Similarly, we also look at the throughput of the CUs. If Algorithm 2 results in the optimal UAV placement r_{C} for the purpose of D_{CU} maximization, the corresponding average throughput per CU is defined as

$$D^{\mathrm{avg}}_{\mathrm{CU}}(r_{\mathrm{C}}) = \frac{D_{\mathrm{CU}}(r_{\mathrm{C}})}{N}. \tag{4.12}$$

Next, we calculate the ratio of these two quantities as

$$\phi = \frac{D^{\mathrm{avg}}_{\mathrm{CU}}(r_{\mathrm{C}})}{D^{\mathrm{avg}}_{\mathrm{D2D}}(r_{\mathrm{D}})}. \tag{4.13}$$

Our objective is to determine the position $s = (x, y, H)$ such that $T(s)$ is minimized, where

$$T(s) = \Big| \frac{D^{\mathrm{avg}}_{\mathrm{CU}}(s)}{D^{\mathrm{avg}}_{\mathrm{D2D}}(s)} - \phi \Big|. \tag{4.14}$$

Here $D^{\mathrm{avg}}_{\mathrm{CU}}(s)$ and $D^{\mathrm{avg}}_{\mathrm{D2D}}(s)$ represents the average throughput per CU and per D2D user

pair, respectively, at $s = (x, y, H)$. Moreover, similar to $r_{\min}$ and $r_{\max}$, we also define the limits of s as $s_{\min} = (x_{s_{\min}}, y_{s_{\min}}, H)$ and $s_{\max} = (x_{s_{\max}}, y_{s_{\max}}, H)$, respectively. Furthermore, we denote the initial value of s as s_0, the mid point of the line joining r_{D} (obtained from Algorithm 1) and r_{C} (obtained from Algorithm 2). In order to find the appropriate s, we propose Algorithm 3, which is largely based on the well-known coordinate search method [18].

4.3.1 Coordinate Search

Coordinate Search is a straightforward and widely used optimization technique that belongs to the class of direct search methods. Unlike gradient-based algorithms, Coordinate Search does not require the calculation of derivatives, making it particularly useful for optimizing functions that are non-differentiable or when gradient information is difficult to obtain.

The main idea behind Coordinate Search is simple: it optimizes a multivariable function by iteratively exploring one coordinate (or variable) at a time, while keeping the others fixed. The search moves along each coordinate direction separately to find an improved solution by testing points in the positive and negative directions of the coordinate axis.

The algorithm begins at an initial guess and proceeds by checking if moving along a coordinate axis by a certain step size results in a better function value. If improvement is found, the point is updated; if not, the algorithm moves on to the next coordinate direction. This process continues iteratively until a stopping criterion, such as a maximum number of iterations or a sufficiently small improvement threshold, is met.

Coordinate Search is simple to implement and easy to understand, making it a popular choice for many engineering and scientific applications. However, its convergence can be slow for high-dimensional problems, as it only searches along one dimension at a time. Nevertheless, it is robust and can handle noisy or discontinuous objective functions where gradient-based methods may fail.

Overall, Coordinate Search offers a practical optimization approach, especially when dealing with complex problems where derivative information is unavailable or unreliable.

The proposed Algorithm 3 works by dividing the xy plane into 360 directions (num_directions), corresponding to the angles from 0° to 360°. Starting with an initial point s_0, the algorithm searches along each direction by adjusting the coordinates in that direction. For each angle, it performs a one-dimensional search, by evaluating the objective function at each step (step_size). The best solution found for each direction

is stored, and the algorithm moves in the direction that minimizes the objective function. Finally the algorithm returns the best position s, which minimizes the objective function.

Since the Coordinate Search algorithm explores the search space by iterating through a finite set of directions, its computational complexity depends primarily on the number of these directions and the maximum number of steps taken along each direction. Here `num_directions` denote the total number of coordinate directions considered, and `max_steps` represent the upper limit on the number of steps taken during the search process. In the worst-case scenario, the algorithm evaluates the objective function at each step along every direction. Therefore, the overall time complexity of the Coordinate Search algorithm can be expressed as $\mathcal{O}(\text{num\_directions} \times \text{max\_steps})$. This linear relationship ensures that the algorithm's running time scales proportionally with both the number of directions and the maximum step count, making it a manageable and predictable method for optimization in many practical applications.

Algorithm 3 Algorithm to find the joint best location

Initialize with initial guess $s_0 = (x_0, y_0, H)$ such that $s_{\min} < s_0 < s_{\max}$, num_directions, step_size and maximum number of steps max_steps.
best_solution $\leftarrow (x_0, y_0)$
best_value $\leftarrow T(s_0)$
for $i = 0$ to num_directions $- 1$ **do**
    $\theta \leftarrow \frac{360}{\text{num\_directions}} \times i$ ▷ Calculate direction angle
    direction $\leftarrow (\cos\theta, \sin\theta)$ ▷ Convert angle to (dx, dy)
    for num_steps $= 1$ to max_steps **do**
        $x_{new} \leftarrow x_0 + \text{direction}[0] \times \text{step\_size}$
        $y_{new} \leftarrow y_0 + \text{direction}[1] \times \text{step\_size}$
        value $\leftarrow T(x_{new}, y_{new})$
        if value $<$ best_value **then**
            best_value $\leftarrow$ value
            best_solution $\leftarrow (x_{new}, y_{new})$
        end if
    end for
end for
return (best_solution)

Chapter 5

Simulation Parameters

To evaluate the performance of the proposed system, extensive simulations are conducted using a well-defined set of parameters, which are summarized below.

The simulation environment spans a square region with dimensions of $300 \times 300\,\mathrm{m}^2$, representing a moderately sized urban communication area. Within this area, a total of $M = 80$ D2D user pairs are randomly distributed. These D2D users communicate directly with each other through a RIS-assisted link. In addition to the D2D pairs, the system also includes $N = 30$ CUs that communicate with a central UAV acting as an aerial base station.

The environment is modeled to include realistic propagation conditions by incorporating 45 randomly placed obstacles, which simulate buildings or other physical obstructions typically found in urban or suburban settings. To support intelligent reflection and improve signal coverage, a RIS comprising $R = 250$ passive reflecting elements is mounted on the UAV. The RIS plays a crucial role in enhancing the quality and reliability of wireless links, particularly in NLoS scenarios [8].

The UAV is assumed to maintain a constant altitude of $H = 25\,\mathrm{m}$, which strikes a balance between coverage area and signal quality. Each D2D transmitter is configured to transmit at a power level of $P_{x_m} = 30\,\mathrm{dBm}$, which is typical for short-range communication devices [19]. To maximize signal gain and mitigate path loss, both the transmit and receive antennas are equipped with directional antennas having a gain of $G_{x_m} = G_{y_m} = 24.5\,\mathrm{dBi}$ [19].

Thermal noise is modeled using a noise power value of $N_0 = -100\,\mathrm{dBm}$, which is a commonly used baseline for millimeter-wave frequency bands. The carrier frequency is set to $28\,\mathrm{GHz}$, reflecting the use of millimeter-wave spectrum often proposed for

next-generation (5G and beyond) wireless communication systems.

Path loss (PL) is modeled differently depending on whether a link is LoS or NLoS. For LoS links, the path loss is defined using a standard model with parameters $\alpha_L = 61.2$ and $\beta_L = 2$ [16], indicating lower attenuation over distance. In contrast, NLoS links exhibit more severe attenuation, modeled with parameters $\alpha_N = 72.0$ and $\beta_N = 2.92$, capturing the additional signal degradation due to scattering, reflection, and diffraction.

These parameters provide a realistic foundation for analyzing the system performance under diverse environmental and operational conditions, allowing for a thorough evaluation of the proposed RIS-UAV-assisted D2D communication network.

Here we list the parameters used for simulation in various scenarios. To ensure a comprehensive evaluation, we consider different parameter settings, which are listed in Table 5.1. The results are examined to assess the effectiveness of the algorithm under different conditions.

Table 5.1: Simulation Parameters

Parameter	**Value**
Communication region	300×300 m^2
Number of D2D pairs users	$M = 80$
Number of CUs	$N = 30$
Number of obstacles	45
Number of reflecting elements	$R = 250$ [8]
UAV height	$H = 25$ m
Transmit power of x_m	$P_{x_m} = 30$ dBm [19]
Gain of the transmit antenna	$G_{x_m} = 24.5$ dBi [19]
Gain of the receive antenna	$G_{y_m} = 24.5$ dBi [19]
Noise power	$N_0 = -100$ dBm
Carrier frequency	28 GHz
PL parameter for LoS link	$\alpha_L = 61.2, \beta_L = 2$ [16]
PL parameter for NLoS link	$\alpha_N = 72.0, \beta_N = 2.92$

Chapter 6

NUMERICAL RESULTS

Here, we evaluate the performance of the proposed algorithm and compare the results against existing benchmarks presented in [13, 12]. In particular, the approach in [13] focuses solely on optimizing the placement of RIS for D2D communications, while [12] optimizes the positioning of UAV to serve cellular users. Unlike these individual approaches, our proposed method jointly optimizes both RIS and UAV positions to support heterogeneous users within a unified framework.

The simulation parameters summarized in Table 5.1 offer a realistic and comprehensive setup for evaluating the efficiency and adaptability of the RIS-mounted UAV-assisted communication system. By systematically varying key environmental and network parameters, such as the number of obstacles and transmit powers, the simulations account for diverse and practical deployment scenarios. Furthermore, we consider both LoS and NLoS path loss models, allowing us to examine the system's behavior.

This evaluation aims to analyze critical performance metrics such as system throughput. The results obtained from these simulations provide valuable insight into how the joint optimization of RIS and UAV components enhances network performance, particularly in dense or obstacle-rich environments. The subsequent sections present a detailed performance comparison in different scenarios, illustrating the robustness and scalability of the proposed framework.

6.1 Convergence of Algorithm 1

Fig. 6.1 demonstrates the convergence of the proposed Algorithm 1, for various values of the Rician parameter K. Specifically, this algorithm provides the optimal location of the RIS in order to maximize the total throughput of the D2D users. Note that the sole

objective of this algorithm is to maximize D_{D2D} without taking care of the CUs present in the environment. This figure illustrates that the proposed algorithm converges in finite time, with the time taken for this purpose being inversely proportional to the learning rate α. Moreover, we also observe that the D_{D2D} achieved is higher for higher values of K, implying the importance of having a LoS between D2D users and the RIS.

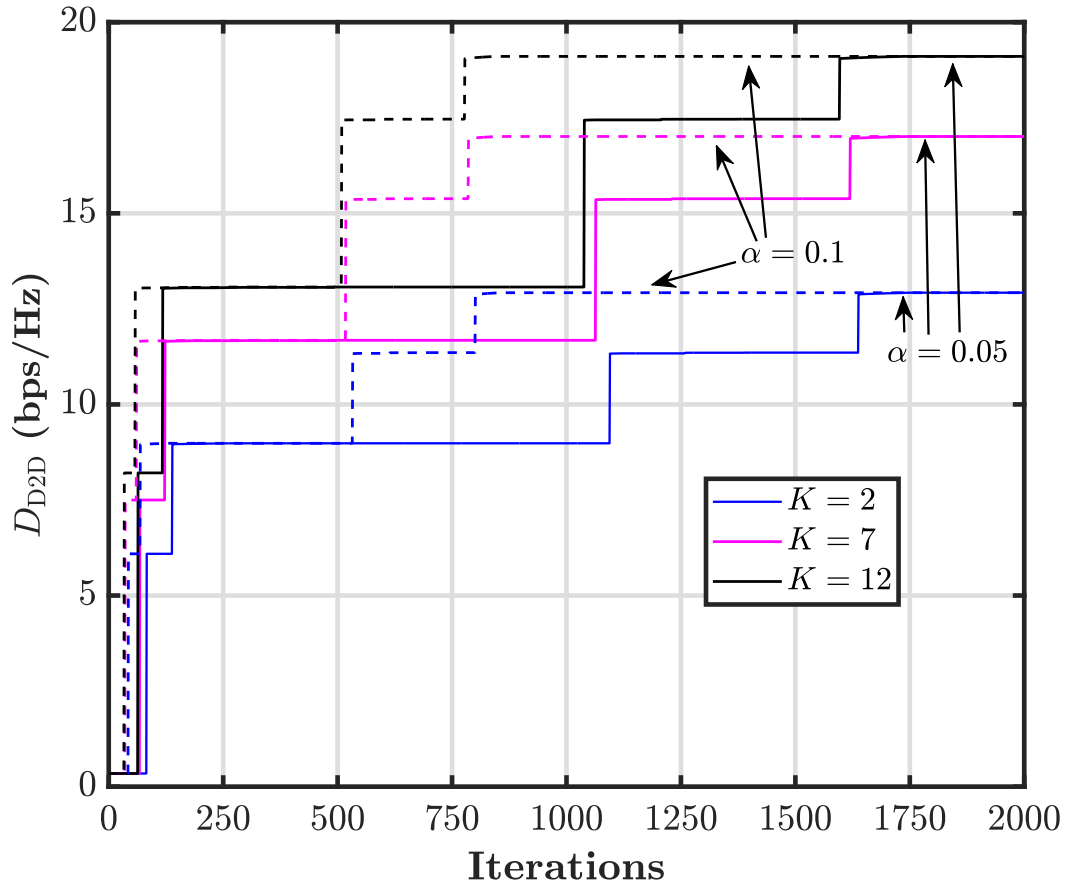

Figure 6.1: Convergence of Algorithm 1.

6.2 Convergence of Algorithm 2

Similarly, Fig. 6.2 depicts the convergence of Algorithm 2, which provides the optimal location of the UAV to maximize the total throughput D_{CU} of the active CUs. Even while the earlier claim regarding the contribution of α to the convergence of Algorithm 1 and the influence of K is still true, we can also see that the system performance is much worse when $K = 0$. This is quite intuitive, as $K = 0$ results in a Rayleigh fading scenario without a LoS link between the CUs and the UAV.

However, our objective is always to place the UAV in such a location, which will result in a LoS link for the maximum possible number of active CUs, if not all.

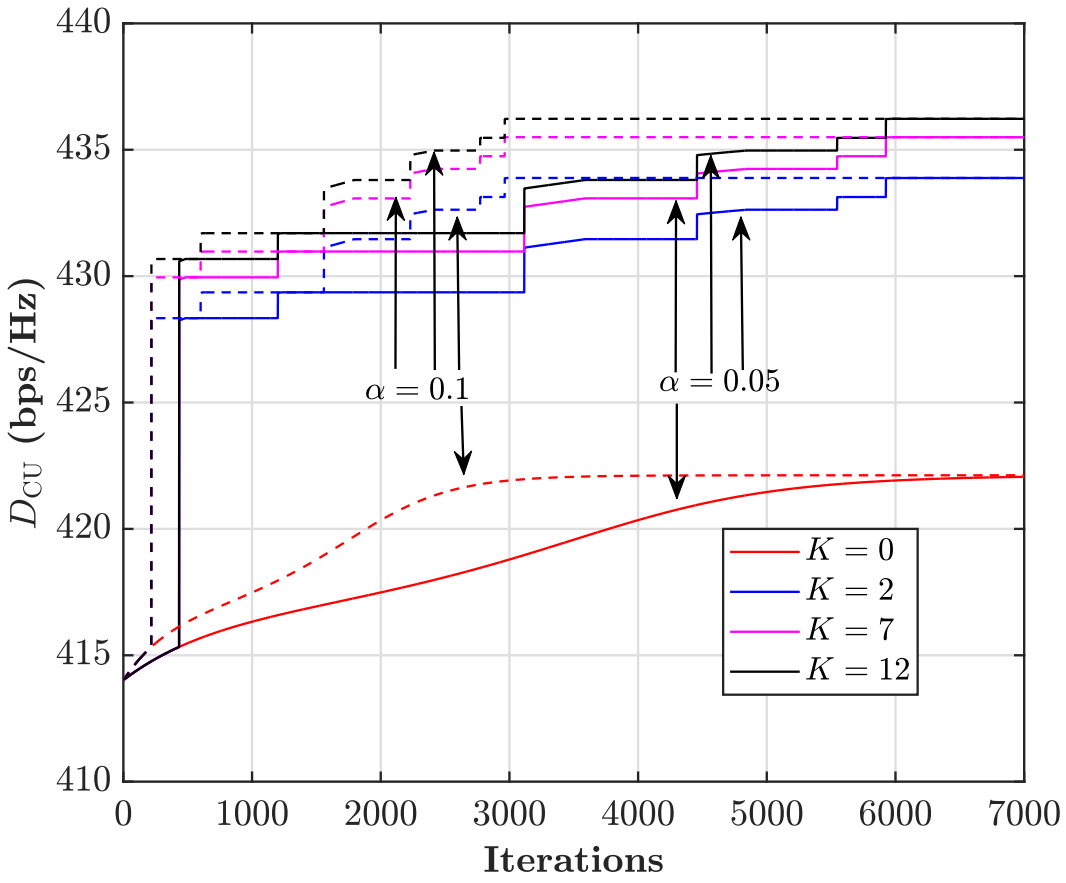

Figure 6.2: Convergence of Algorithm 2.

6.3 Impact of obstacles on the system performance

It is important to note that, while Algorithm 1 and Algorithm 2 may provide different optimal RIS and UAV locations, it is practically not feasible. This is because the RIS is placed on top of the UAV. Therefore, we search for a position, which enhances the net throughput of both the D2D users as well as the CUs at the same time. Algorithm 3 finds this position. In Fig. 6.3, we investigate the impact of the obstacles present in the environment on the net throughput D_{net} obtained by (3.10). In this figure, $D_{\mathrm{net}}^{\mathrm{opt}}$ represents the net throughput computed based on the optimal location obtained by Algorithm 3. Here, $D_{\mathrm{D2D}}^{\mathrm{opt}}$ and $D_{\mathrm{CU}}^{\mathrm{opt}}$ represent the net throughput obtained by [13] and [12], respectively. According to [13], we first determine the best location for D2D

users and compute D_{D2D}. We then compute D_{CU} for the CUs using the same location obtained for the D2D users. Finally, we compute D_{net} by using (3.10) and denote it by $D_{\text{D2D}}^{\text{opt}}$. In the same way, we compute $D_{\text{CU}}^{\text{opt}}$ based on the optimal location for CUs as in [12].

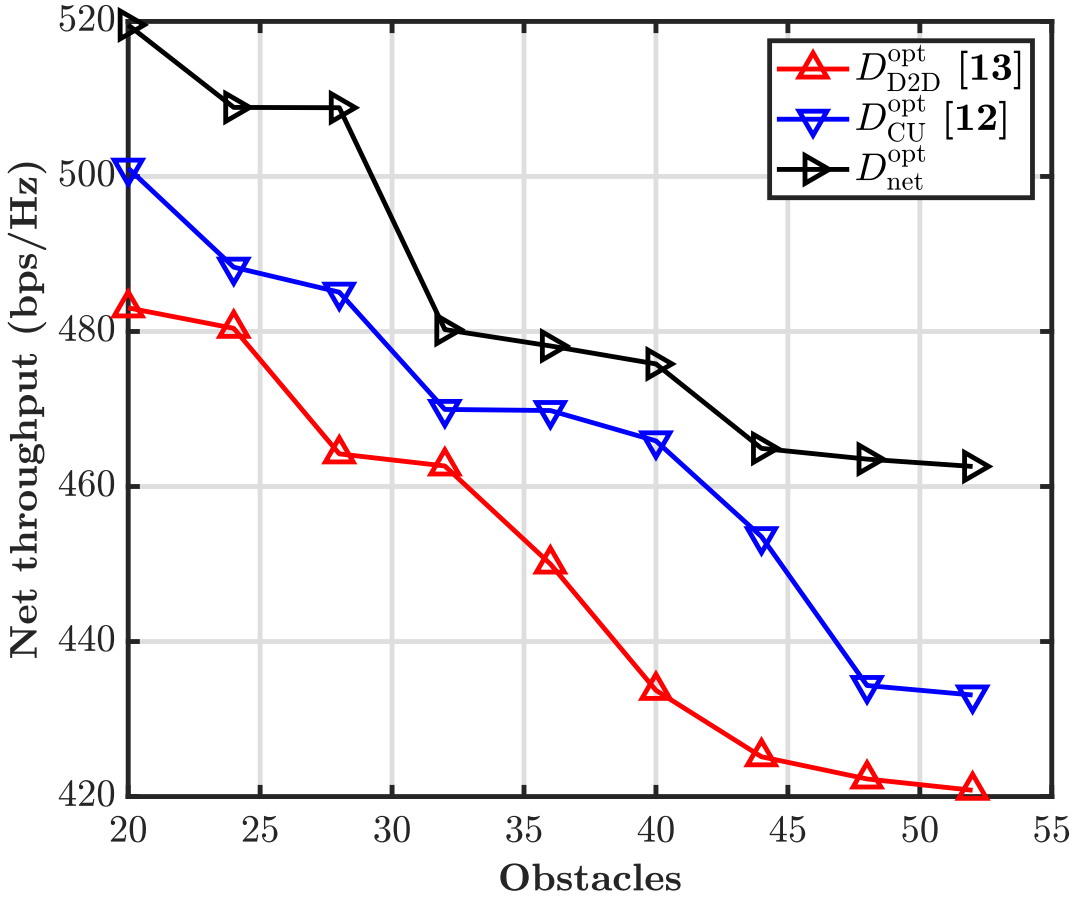

Figure 6.3: Impact of obstacles on the system performance.

We observe from the figure 6.3 that irrespective of the framework, the net throughput decreases with increasing obstacles, which is intuitive. However, it is interesting to see that, $D_{\text{net}}^{\text{opt}}$ is always greater than the other schemes, which aim to individually provide greater throughput to the D2D users or the CUs. This brings out the novelty of our proposed framework, as to individually maximizing D_{D2D} or D_{CU} does not necessarily imply enhancing the total system throughput. Algorithm 3 outperforms the others, as it considers the best location for both the D2D users and the CUs.

6.4 Impact of obstacles on the system fairness

Finally, we look at the impact of obstacles on the Jain's fairness index [20]. Jain's Fairness Index (JFI) is a widely used metric to evaluate the fairness of resource allocation among multiple users or entities in a system.

6.4.1 Jain's Fairness Index

Definition:

Given a set of resource allocations $x_1, x_2, \ldots, x_n$ to n users, Jain's Fairness Index (JFI) is defined as:

$$\text{JFI} = \frac{(\sum_{i=1}^{n} x_i)^2}{n \cdot \sum_{i=1}^{n} x_i^2}$$

Jain's Fairness Index is a widely used metric to evaluate the fairness of resource allocation among multiple users or entities. It provides a normalized value between $\frac{1}{n}$ and 1, where n is the number of users. A JFI value of 1 indicates perfect fairness, meaning all users receive equal shares, while a value closer to $\frac{1}{n}$ reflects high inequality in distribution. The index is scale-invariant and symmetric, making it suitable for comparing allocation strategies regardless of the units or user ordering. It is commonly used in networking, wireless communications, and systems resource management.

Properties:

- **Range:** $\frac{1}{n} \leq \text{JFI} \leq 1$
  - JFI $= 1$: Perfect fairness (all users get equal allocation).
  - JFI $= \frac{1}{n}$: Maximum unfairness (only one user gets all the resources).
- **Scale Invariant:** It depends only on the relative values of x_i, not their absolute scale.
- **Symmetric:** The index is unaffected by permuting the order of users.

Based on the method described in [13], we first find the best location for the D2D users and calculate D_{D2D}. Using this same location, we then compute D_{CU}. With both values, we calculate Jain's Fairness Index, which we refer to as $\mathcal{J}_{\text{D2D}}$. In a similar way, following the approach in [12], we determine the optimal location for the CUs and, from this location, calculate both D_{D2D} and D_{CU}. Using these values, we compute the fairness index, denoted as $\mathcal{J}_{\text{CU}}$. Finally, using our proposed method (Algorithm 3), we calculate the fairness index, which we denote as $\mathcal{J}_{\text{opt}}$.

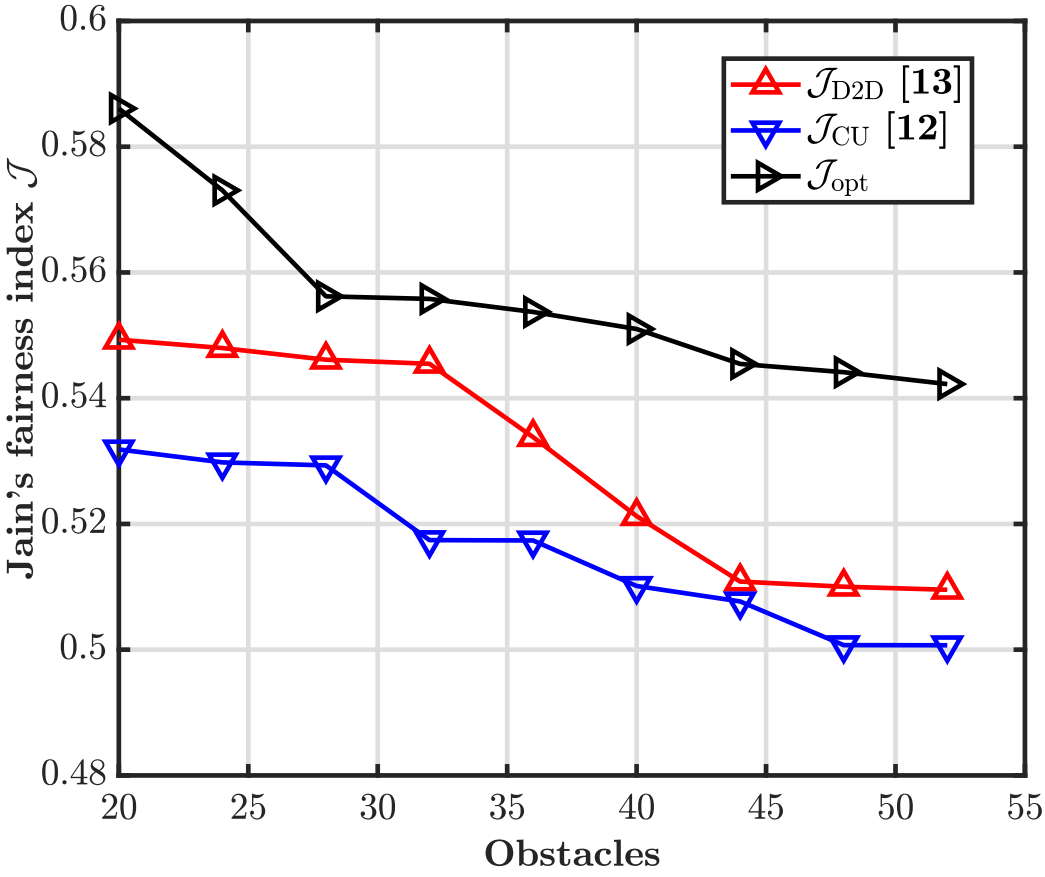

Figure 6.4: Impact of obstacles on the system fairness.

In figure 6.4, we observe that Algorithm 3 results in the best performance among the existing benchmarks [13], [12]. In other words, our approach is fair to both the D2D pairs and the CUs.

6.5 Impact of obstacles on the average system performance

In Figure 6.5, we investigate the impact of the obstacles present in the environment on the average performance of the system. Suppose that there are M D2D pairs and N CUs being served at the same time. Therefore, based on the Algorithm 3 and (3.10), we optimally evaluate the quantity

$$D_{net}^{opt} = \frac{1}{2}\left(\frac{D_{D2D}}{M} + \frac{D_{CU}}{N}\right). \tag{6.1}$$

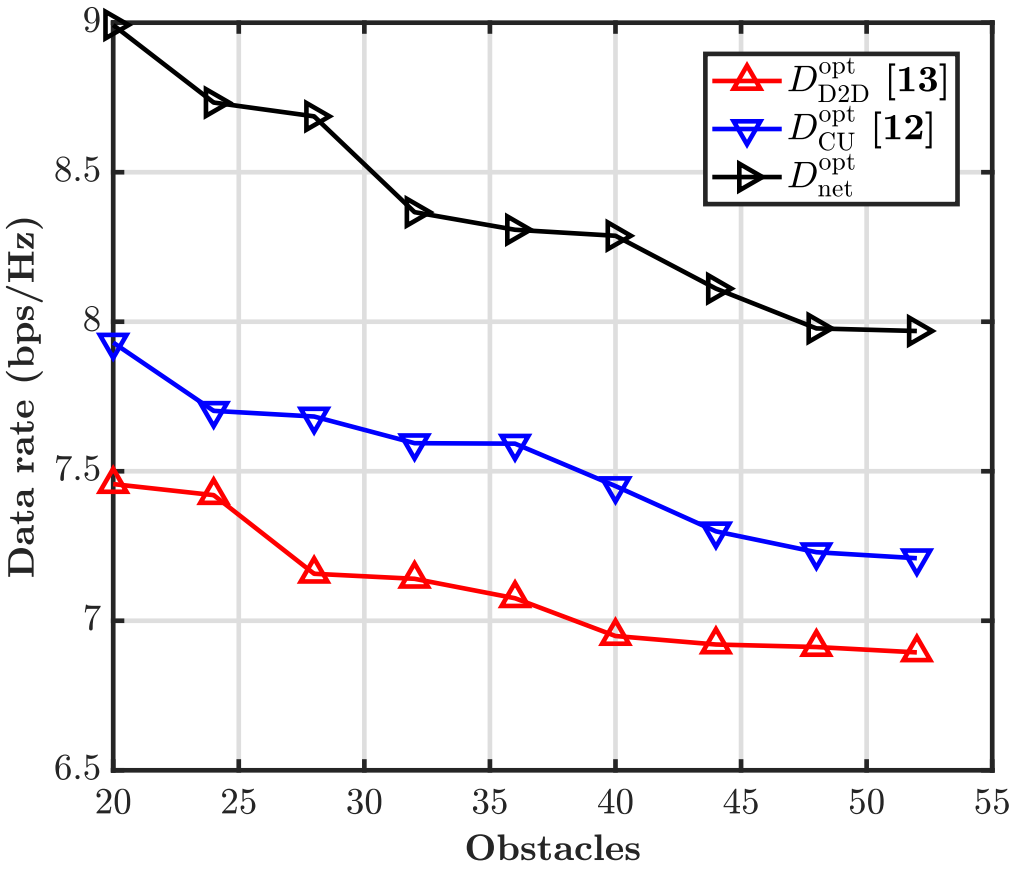

Figure 6.5: Impact of obstacles on the average system performance.

In addition, we also consider the following cases.

- Find optimal location for the D2D users (Algorithm 1) and use this same location to serve the CUs, resulting in D^{opt}_{D2D}.
- Find optimal location for the CUs (Algorithm 2) and use this same location to serve the D2D users, resulting in D^{opt}_{CU}.

This helps us to bring out the novelty of our proposed framework, as to individually maximizing D_{D2D} or D_{CU} does not necessarily imply enhancing the total system throughput. We observe from the figure 6.5 that irrespective of the framework, the data rate decreases with increasing obstacles, which is intuitive. However, it is interesting to see that, D^{opt}_{net} is always greater than the other schemes, which aim to individually provide greater throughput to the D2D users or the CUs.

6.6 Impact of transmission power on the system performance

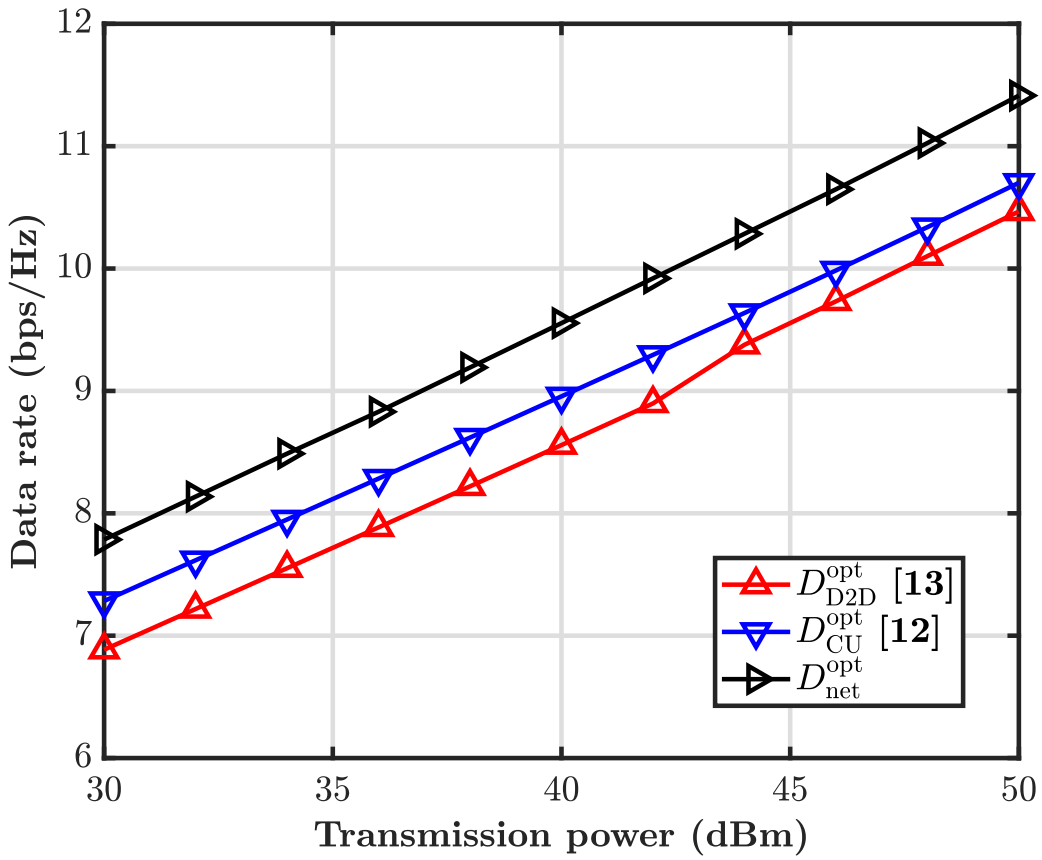

Figure 6.6: Impact of transmission power on the system performance.

Figure 6.6 demonstrates the impact of the transmission power of the users on the system performance. We observe, that all the schemes result in better throughput with increasing trans mission power, which is again intuitive. But it is interesting to observe that for all transmission powers, the proposed scheme outperforms the other two. The reason for this attributed to the fact as discussed earlier with respect to Figure 6.5.

Chapter 7

CONCLUSION

In this work, we investigate the problem of optimal placement for RIS-mounted UAVs in wireless networks. Our study focuses on two distinct types of users: D2D pairs and CUs. Unlike previous approaches that optimize for only one user type, we propose novel algorithms that jointly maximize the overall system throughput by considering both user groups simultaneously. Through extensive numerical simulations, we demonstrate that the proposed framework not only achieves higher throughput but also ensures improved fairness among users. The results clearly show the advantages of our approach when compared to existing benchmark methods, making it a promising solution for enhancing network performance in practical RIS-assisted UAV deployments.

This work addresses the critical challenge of optimal deployment for RIS-mounted UAV networks, focusing on enhancing wireless communication performance in environments with both D2D pairs and CUs. By developing algorithms that jointly consider these two user types, our approach aims to maximize the overall system throughput while maintaining fairness across the network. The comprehensive numerical analysis validates the effectiveness of the proposed framework, demonstrating significant improvements over existing benchmark schemes in terms of throughput and fairness. These results highlight the practical potential of RIS-mounted UAVs to dynamically adapt to complex network conditions and user distributions. Moving forward, this research lays a strong foundation for future studies that may incorporate additional factors such as mobility, energy constraints, and real-time adaptive algorithms, ultimately advancing the design of more intelligent and efficient wireless communication systems.

Furthermore, our work provides strong evidence that joint optimization—considering

all user types instead of treating them separately—is more effective in real-world applications. As wireless networks become denser and more diverse, such joint strategies will become increasingly necessary.

In summary, this research has proposed and validated a new approach to improving wireless communication through the optimal placement of RIS-mounted UAVs. By jointly considering D2D pairs and CUs, we have shown that it is possible to significantly improve both throughput and fairness across the network. The results serve as a strong foundation for future exploration in this area, with many exciting possibilities for further development.

Our work contributes to the ongoing evolution of wireless networks, pushing toward more intelligent, flexible, and user-aware communication systems. As the demand for faster and more reliable connectivity continues to grow, such advanced solutions will play a critical role in shaping the future of global communications.

Bibliography

[1] Ericsson Mobility Report. [Online]. Available: https://www.ericsson.com/en/mobility-report/reports/november-2024. Nov. 2024.

[2] E. Basar, M. Di Renzo, J. De Rosny, M. Debbah, M.-S. Alouini, and R. Zhang. "Wireless communications through reconfigurable intelligent surfaces". In: *IEEE Access* 7 (2019), pp. 116753–116773.

[3] S. Tewes, M. Heinrichs, R. Kronberger, and A. Sezgin. "IRS-enabled breath tracking with colocated commodity WiFi transceivers". In: *IEEE Internet Things J.* 10.8 (Aug. 2022), pp. 6870–6886.

[4] K. Z. Ghafoor, L. Kong, S. Zeadally, A. S. Sadiq, G. Epiphaniou, M. Hammoudeh, A. K. Bashir, and S. Mumtaz. "Millimeter-wave communication for internet of vehicles: status, challenges, and perspectives". In: *IEEE Internet Things J.* 7.9 (Sept. 2020), pp. 8525–8546.

[5] L. Sau, P. Mukherjee, and S. C. Ghosh. "DRAMS: Double-RIS assisted multihop routing scheme for device-to-device communication". In: *Comput. Commun.* 220 (Apr. 2024), pp. 52–63.

[6] S. Zeng et al. "Reconfigurable intelligent surface (RIS) assisted wireless coverage extension: RIS orientation and location optimization". In: *IEEE Commun. Lett.* 25.1 (Jan. 2020), pp. 269–273.

[7] Z. Kang, C. You, and R. Zhang. "Double-active-IRS aided wireless communication: Deployment optimization and capacity scaling". In: *IEEE Wireless Commun. Lett.* 12.11 (Nov. 2023), pp. 1821–1825.

[8] L. Sau, P. Mukherjee, and S. C. Ghosh. "Priority-aware grouping-based multihop routing scheme for RIS-assisted wireless networks". In: *IEEE Trans. Network Sci. Eng.* 12.2 (Mar. 2025), pp. 1172–1185.

[9] Q. Wu et al. "A comprehensive overview on 5G-and-beyond networks with UAVs: From communications to sensing and intelligence". In: *IEEE J. Sel. Areas Commun.* 39.10 (Oct. 2021), pp. 2912–2945.

[10] M. Gapeyenko, D. Moltchanov, S. Andreev, and R. W. Heath. “Line-of-sight probability for mmWave-based UAV communications in 3D urban grid deployments”. In: *IEEE Trans. Wireless Commun.* 20.10 (Oct. 2021), pp. 6566–6579.

[11] T. Shafique, H. Tabassum, and E. Hossain. “Optimization of Wireless Relaying With Flexible UAV-Borne Reflecting Surfaces”. In: *IEEE Trans. Commun.* 69.1 (Jan. 2021), pp. 309–325.

[12] M.-H. T. Nguyen, E. Garcia-Palacios, T. Do-Duy, O. A. Dobre, and T. Q. Duong. “UAV-Aided Aerial Reconfigurable Intelligent Surface Communications With Massive MIMO System”. In: *IEEE Trans. Cognit. Commun. Networking* 8.4 (Dec. 2022), pp. 1828–1838.

[13] P. Wang et al. “UAV-Assisted Vehicular Communication System Optimization With Aerial Base Station and Intelligent Reflecting Surface”. In: *IEEE Trans. Intell. Veh.* (2023). early access.

[14] Y. Yang, B. Zheng, S. Zhang, and R. Zhang. “Intelligent reflecting surface meets OFDM: Protocol design and rate maximization”. In: *IEEE Trans. Commun.* 68.7 (July 2020), pp. 4522–4535.

[15] M. Samir, S. Sharafeddine, C. M. Assi, T. M. Nguyen, and A. Ghrayeb. “UAV Trajectory Planning for Data Collection from Time-Constrained IoT Devices”. In: *IEEE Trans. Wireless Commun.* 19.1 (Jan. 2020), pp. 34–46.

[16] F. Li, C. He, X. Li, J. Peng, and K. Yang. “Geometric analysis-based 3D anti-block UAV deployment for mmWave communications”. In: *IEEE Commun. Lett.* 26.11 (Nov. 2022), pp. 2799–2803.

[17] N. Mensi, D. B. Rawat, and E. Balti. “Gradient Ascent Algorithm for Enhancing Secrecy Rate in Wireless Communications for Smart Grid”. In: *IEEE Trans. Green Commun. Networking* 6.1 (Mar. 2022), pp. 107–116.

[18] E. Frandi and A. Papini. “Coordinate search algorithms in multilevel optimization”. In: *Optim. Methods Software* 29.5 (Nov. 2013), pp. 1020–1041.

[19] M. R. Akdeniz, Y. Liu, M. K. Samimi, S. Sun, S. Rangan, T. S. Rappaport, and E. Erkip. “Millimeter wave channel modeling and cellular capacity evaluation”. In: *IEEE J. Sel. Areas Commun.* 32.6 (June 2014), pp. 1164–1179.

[20] A. B. Sediq, R. H. Gohary, R. Schoenen, and H. Yanikomeroglu. “Optimal Tradeoff Between Sum-Rate Efficiency and Jain’s Fairness Index in Resource Allocation”. In: *IEEE Trans. Wireless Commun.* 12.7 (July 2013), pp. 3496–3509.